

Polyethylene and Semiconducting Polymer Blends for the Fabrication of Organic Field-Effect Transistors: Balancing Charge Transport and Stretchability

Piumi Kulatunga, Nastaran Yousefi and Simon Rondeau-Gagné *

Department of Chemistry and Biochemistry, University of Windsor, Windsor, ON N9B 3P4, Canada;
kulatun@uwindsor.ca (P.K.); nastaran.yousefi@uwindsor.ca (N.Y.)

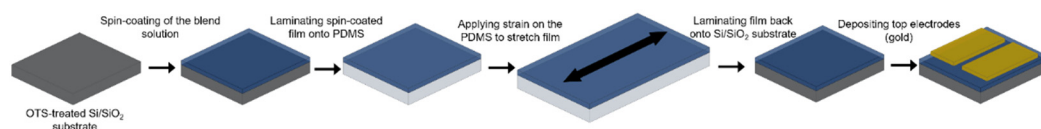
* Correspondence: srondeau@uwindsor.ca

P(DPPTVT) Synthesis

A microwave vessel equipped with a stir bar was charged with (E)-1,2-bis(5-(trimethylstannyl)thiophen-2-yl)ethene (45.78 mg, 0.088 mmol), 3,6-bis(5-bromothiophen-2-yl)-2,5-bis(2-decyltetradecyl)-2,5-dihydropyrrolo[3,4-c]pyrrole-1,4-dione (100 mg, 0.088 mmol), and degassed chlorobenzene (3.5 mL). It was then bubbled with N₂ gas for 30 minutes and Pd₂(dba)₃ and P(*o*-tolyl)₃ were added quickly. The vessel was immediately sealed with a snap cap and kept for 3 days at 120 °C. After reaction completion, the polymer was end-capped with trimethyl(phenyl)tin (21.2 mg, 0.088 mmol) and bromobenzene (13.8 mg, 0.088 mmol), successively. The reaction mixture was then cooled to room temperature and dissolved in TCE. This solution was then precipitated in methanol and the solid was collected by filtration into a glass thimble. The contents of the thimble were then extracted in a Soxhlet extractor with methanol, acetone, hexane, and finally chlorobenzene. The chlorobenzene fraction was concentrated and reprecipitated in methanol, followed by filtration and drying under vacuum. Molecular weight was estimated from high-temperature SEC.

Transfer-Printed Organic Field-Effect Transistor Fabrication

To measure the charge mobilities upon stretching, the lamination procedure was used to transfer the semiconducting polymer films onto PDMS. Scheme 1 shows the sequential steps taken in the process of OFET fabrication for stretched films.



Scheme S1. The process of transfer-printed organic field-effect transistor fabrication, depicting the order of steps (left to right).

Measurement of Dichroic Ratios

To measure the dichroic ratio, pre-stretched thin films on PDMS were fixed on a glass substrate using a double-sided adhesive tape and placed in the UV-vis light pathway in the spectrometer for absorbance measurements. The dichroic ratio was calculated by dividing the absorbance intensity at 0° (light polarized parallel to the stretching direction) and 90° (light polarized perpendicular to the stretching direction).

Measurement of Crack Width

Polymer blend solutions were spin-casted on polystyrene sulfonate (PSS)-coated glass slides prepared by spin-coating a 50 mg mL⁻¹ aqueous solution of PSS in water. Polydimethylsiloxane (PDMS) was used as the elastomer substrate mixed at a base to cross-linker ratio of 15:1, and crosslinked at 70 °C overnight. PDMS strips were placed on the coated PSS glass slide with polymer blend and then immersed in water for 10 min. Consequently, the PSS layer was dissolved, and thin film was attached to the PDMS. Then, PDMS was stretched to the selected strain elongation using a microscope stretcher. In the final step, the stretched thin films were transferred onto the Si wafers and characterized by optical microscopy.

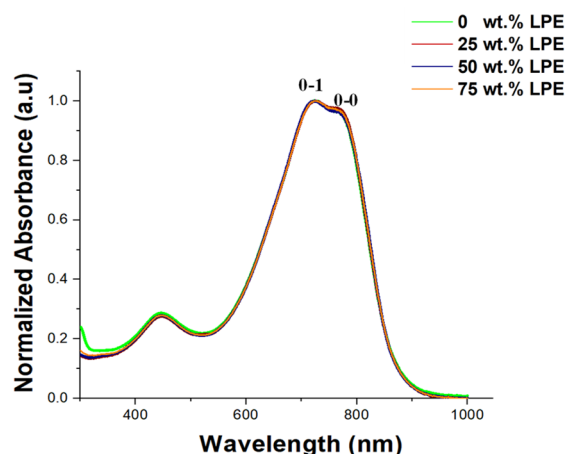


Figure S1. UV-vis spectra of P(DPPTVT):LPE blend solutions. Absorbance is normalized based on the intensity of the 0–1 peak.

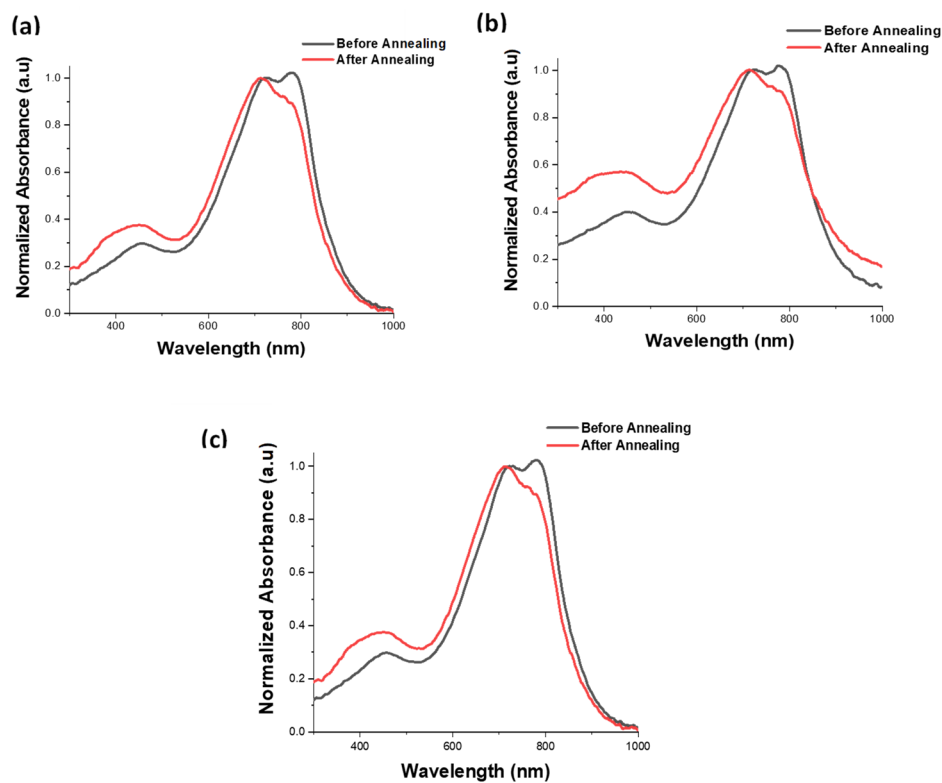


Figure S2. UV-vis spectra of P(DPPTVT):LPE thin films with (a) 0 wt.% LPE, (b) 25 wt.% LPE, and (c) 50 wt.% LPE, before and after thermal annealing at 150 °C. Absorbance is normalized based on the intensity of the 0–1 peak.

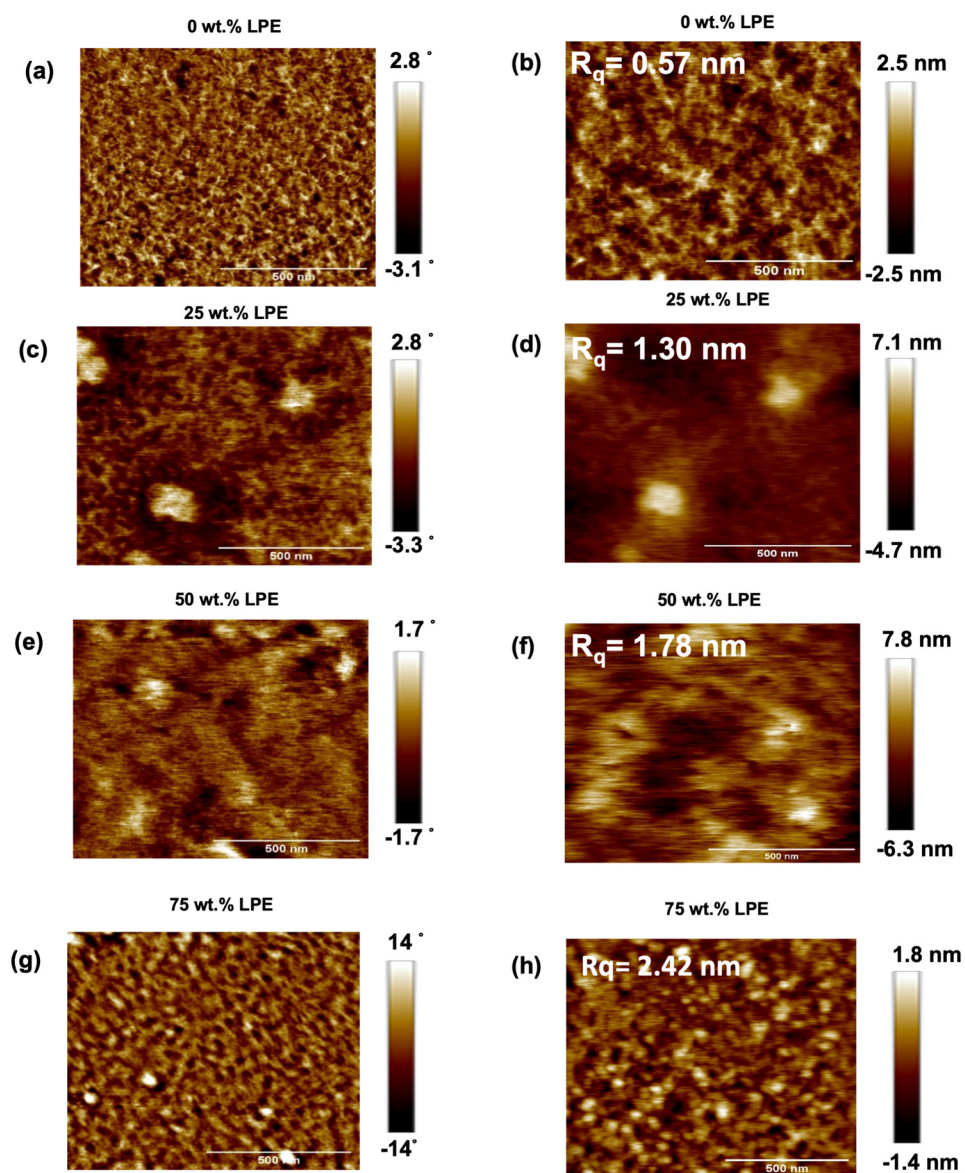


Figure S3. Atomic force microscopy images (a), (c), (e), and (g): phase images; and (b), (d), (f), and (h): height images) of P(DPPTVT):LPE thin films fabricated via spin-casting of solutions in chloro-benzene, before thermal annealing. Scale bar is 500 nm.

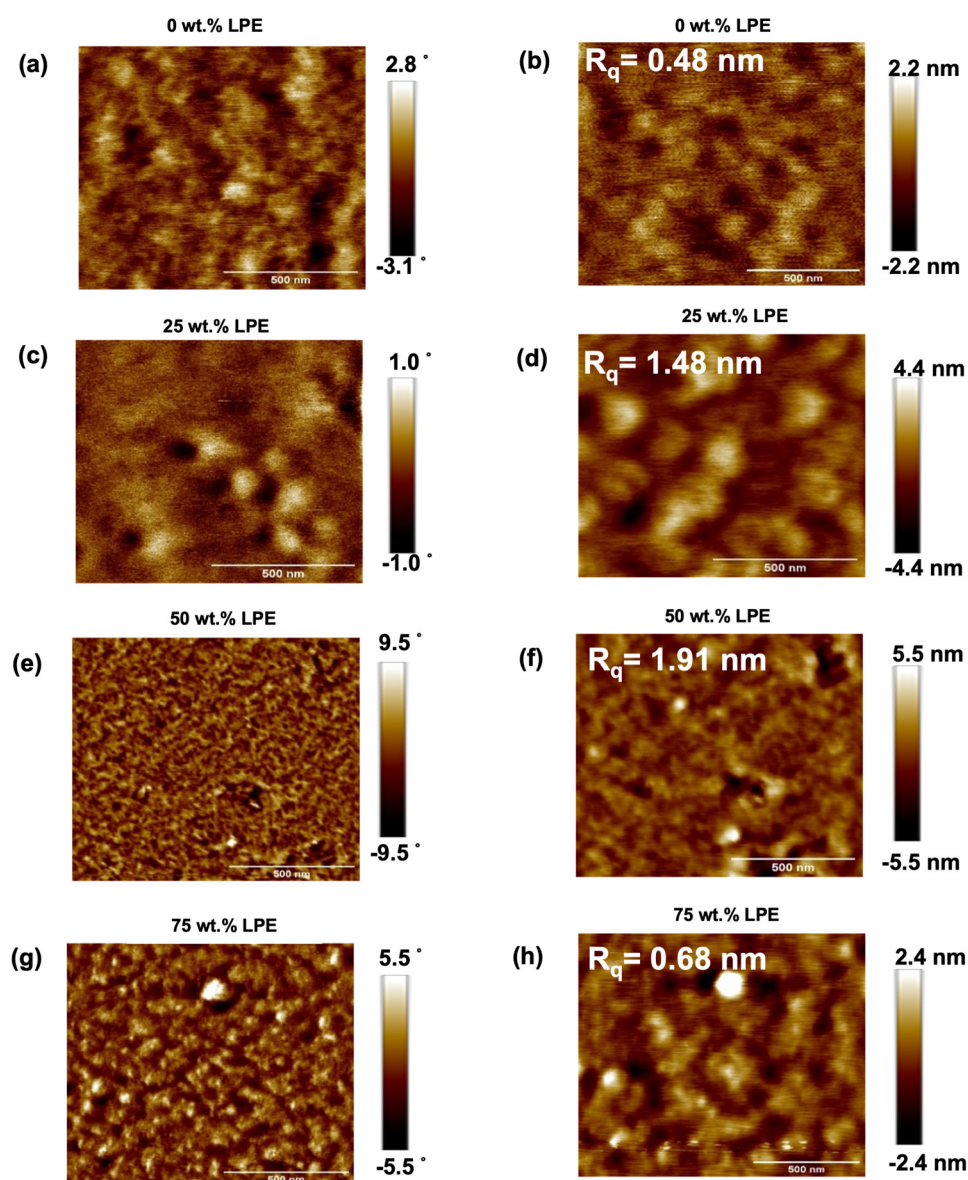


Figure S4. Atomic force microscopy images (a), (c), (e), and (g): phase images; and (b), (d), (f), and (h): height images) of P(DPPTVT):LPE thin films fabricated via spin-casting of solutions in chloro-benzene, after thermal annealing at 90 °C. Scale bar is 500 nm.

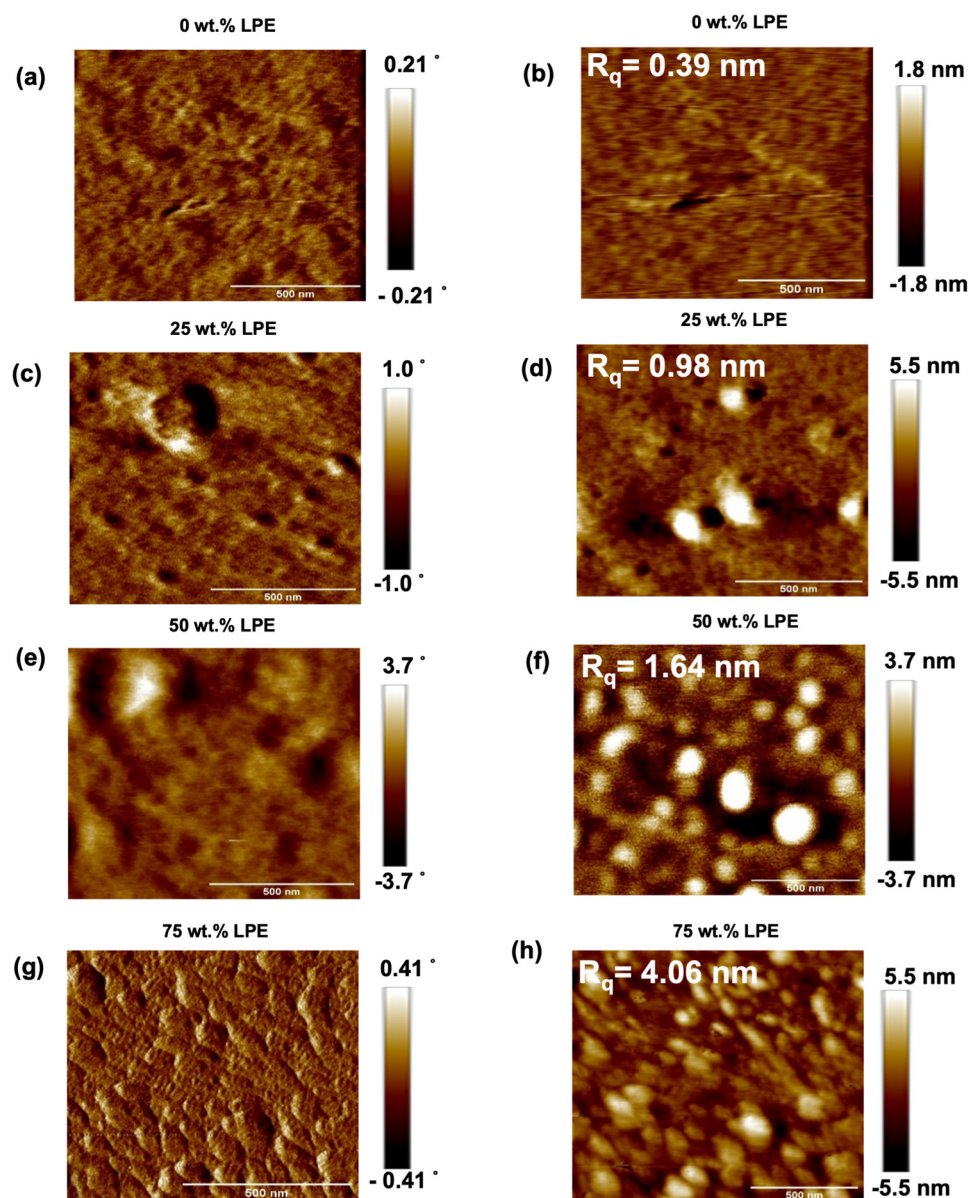


Figure S5. Atomic force microscopy images (a), (c), (e), and (g): phase images; and (b), (d), (f), and (h): height images) of P(DPPTVT):LPE thin films fabricated via spin-casting of solutions in chloro-benzene, after thermal annealing at 150 °C. Scale bar is 500 nm.

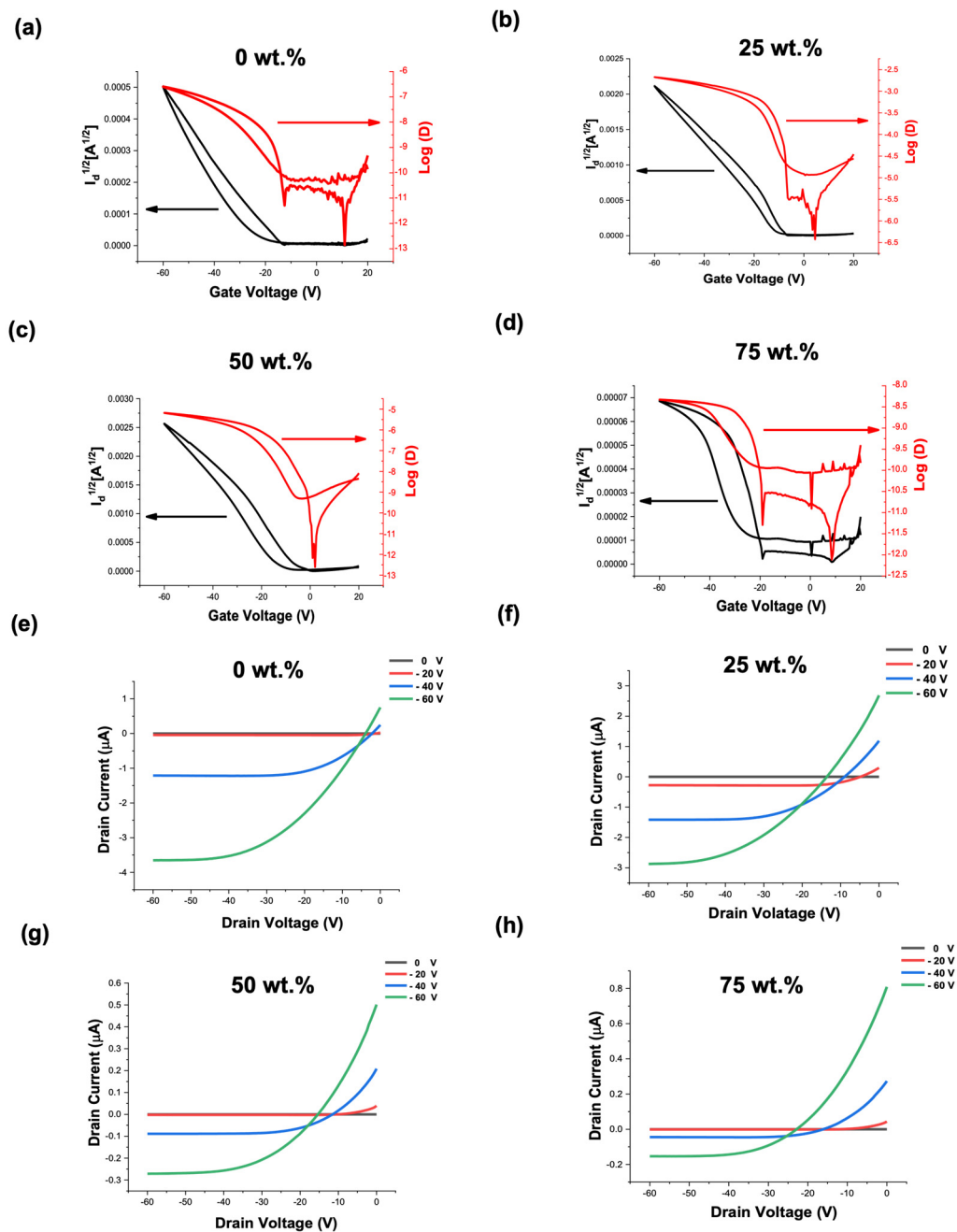


Figure S6. Transfer (a)–(d) and output (e)–(h) curves for OFET devices fabricated using 0–75 wt.% LPE before thermal annealing ($V_d = -60\text{V}$).

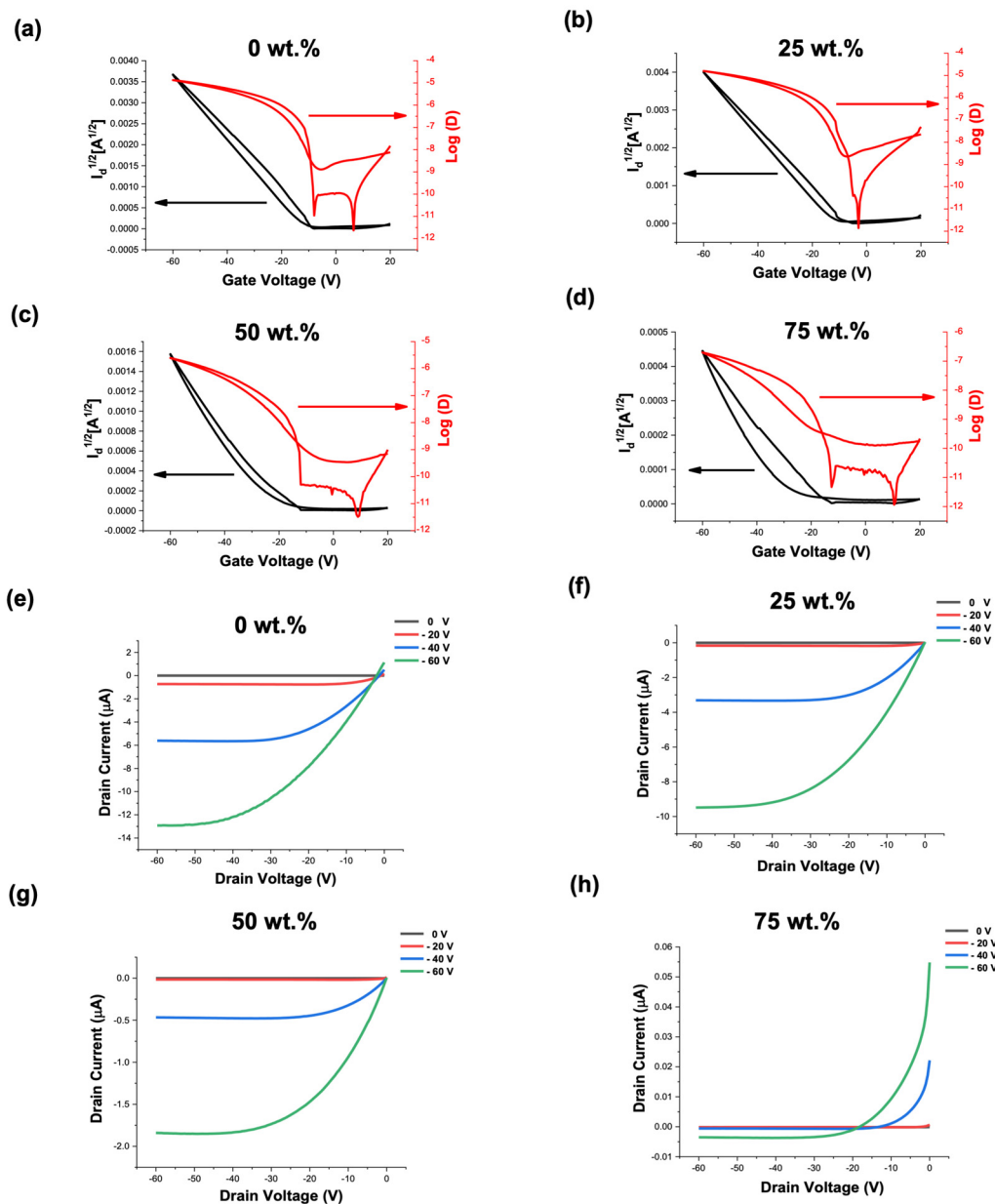


Figure S7. Transfer (a)–(d) and output (e)–(h) curves for OFET devices fabricated using 0–75 wt.% LPE after thermal annealing at 90 °C for 30 min ($V_d = -60\text{V}$).

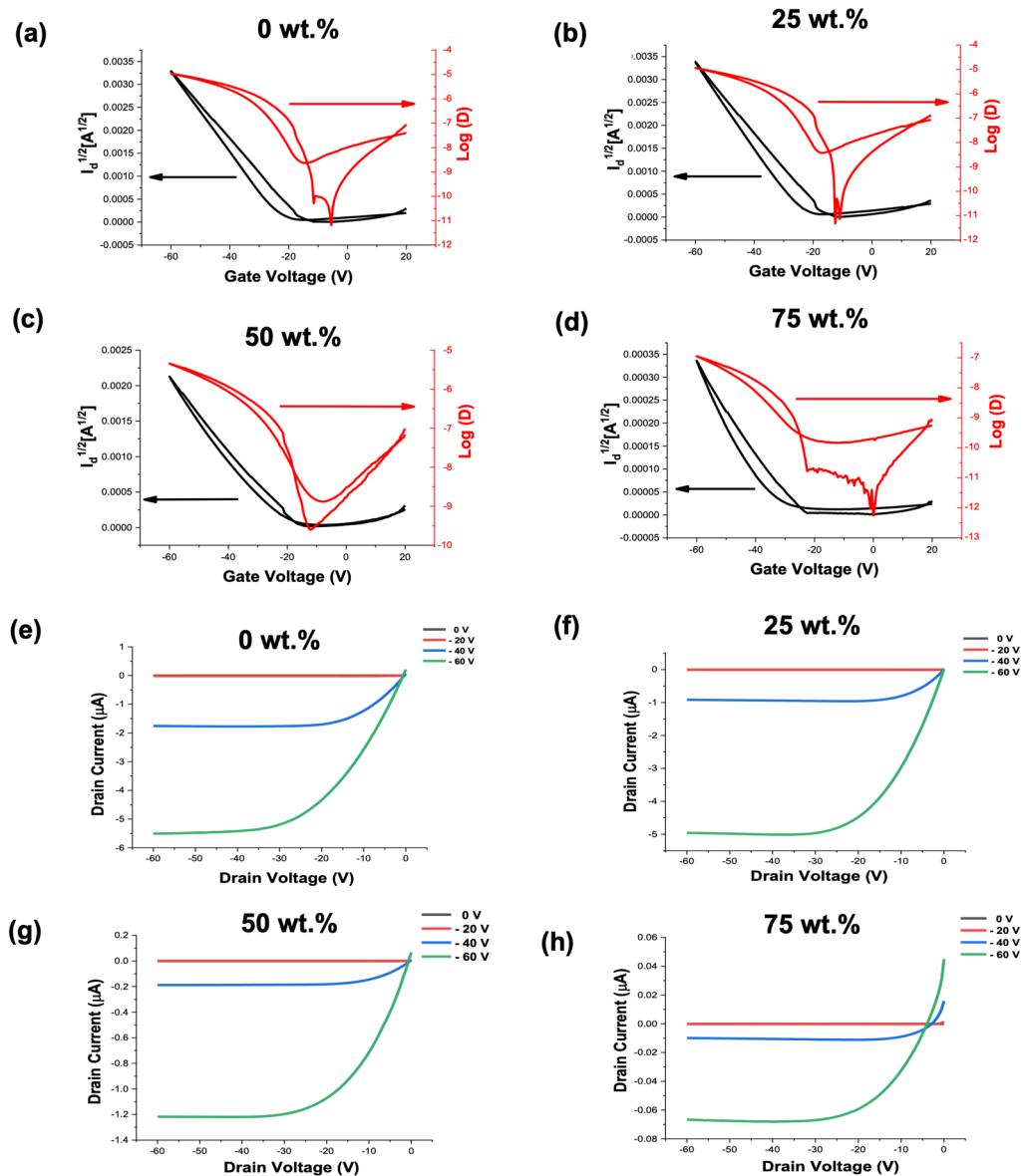


Figure S8. Transfer (a)–(d) and output (e)–(h) curves for OFET devices fabricated using 0–75 wt.% LPE after thermal annealing at 150 °C for 30 min ($V_d = -60$ V).

Table S1. Average (μ_h^{avg}) and maximum hole mobilities (μ_h^{max}), threshold voltages (V_{th}), and I_{on}/I_{off} ratios for OFETs fabricated using polymer blends (0–75 wt.% LPE) before and after thermal annealing. The device performances were averaged from 10 devices and W/L represents channel width/length.

Sample	Annealing Temperature (°C)	W/L	μ_h^{avg}/μ_h^{max} ($cm^2 V^{-1} s^{-1}$)	I_{on}/I_{off}^{avg}	V_{th}^{avg} (V)
0 wt. %	As cast		$0.039 \pm 0.002/0.052$	10^6	0.34 ± 10.45
	90	6.66	$0.123 \pm 0.005/0.140$	10^6	-4.17 ± 1.95
	150		$0.126 \pm 0.007/0.1482$	10^6	-15.98 ± 3.12
25 wt. %	As cast		$0.032 \pm 0.001/0.039$	10^6	3.70 ± 1.39
	90	6.66	$0.139 \pm 0.002/0.146$	10^6	-11.63 ± 2.66
	150		$0.151 \pm 0.003/0.161$	10^6	-21.30 ± 3.49
50 wt. %	As cast		$0.006 \pm 0.002/0.024$	10^6	-17.8 ± 2.27
	90	6.66	$0.045 \pm 0.003/0.055$	10^6	-19.14 ± 3.85
	150		$0.065 \pm 0.005/0.084$	10^6	-23.98 ± 3.37
75 wt. %	As cast		$0.0012 \pm 0.0003/0.0038$	10^3	-17.26 ± 3.01
	90	6.66	$0.0008 \pm 0.0004/0.0032$	10^3	-16.55 ± 2.93
	150		$0.0007 \pm 0.0005/0.0027$	10^3	-28.33 ± 2.2

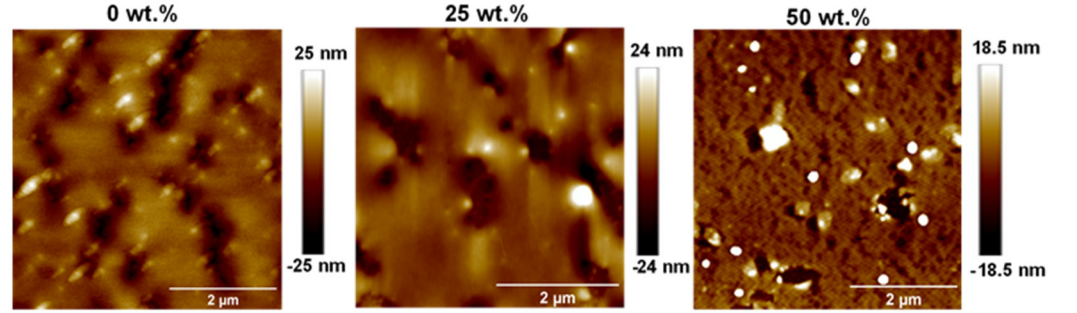


Figure S9. Atomic force microscopy images (height) of P(DPPTVT): LPE blends at 100% strain before thermal annealing. The scale bar is 2.0 μm .

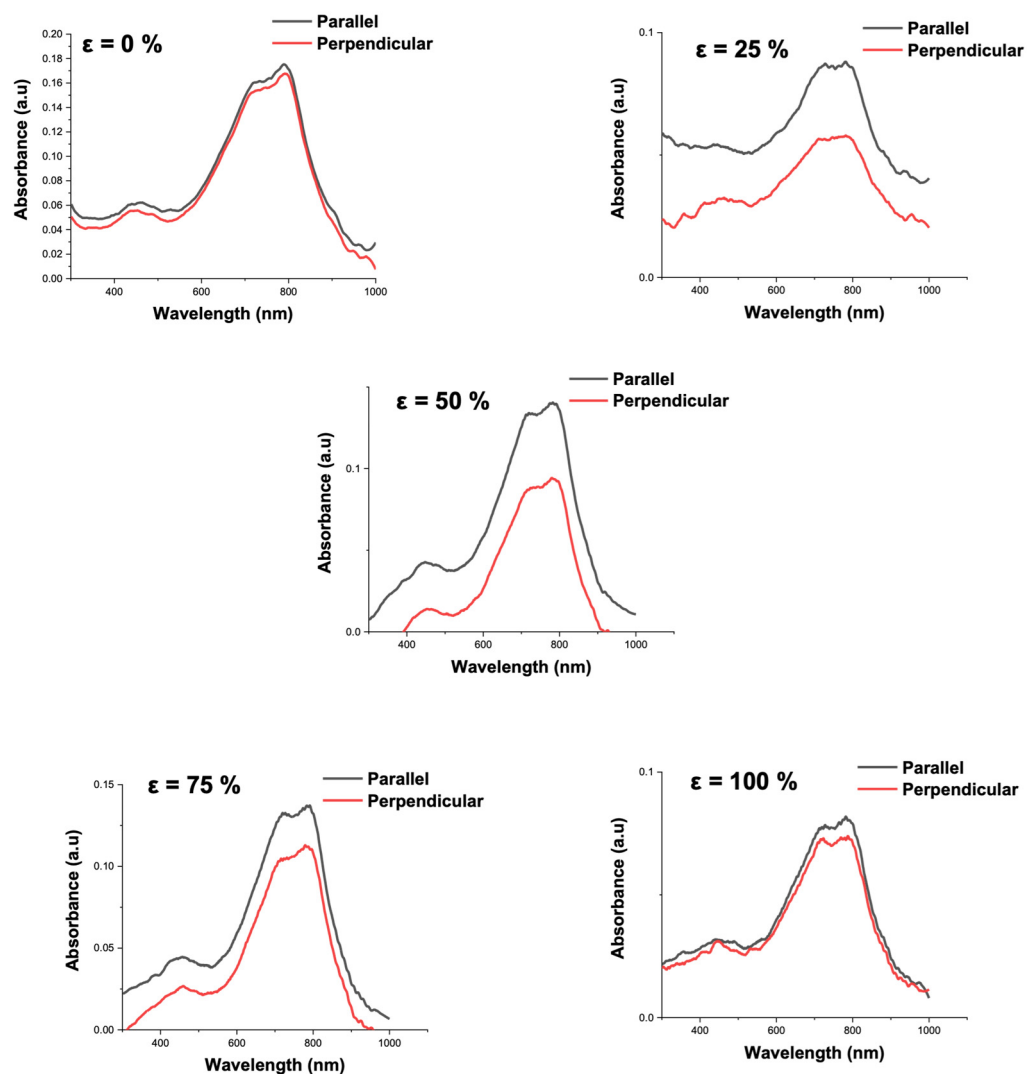


Figure S10. Polarized UV-vis spectra of P(DPPTVT) thin films with 0 wt.% LPE stretched at different percent strains with the polarization direction of light parallel (0° , black trace) and perpendicular (90° , red trace) to the stretching direction.

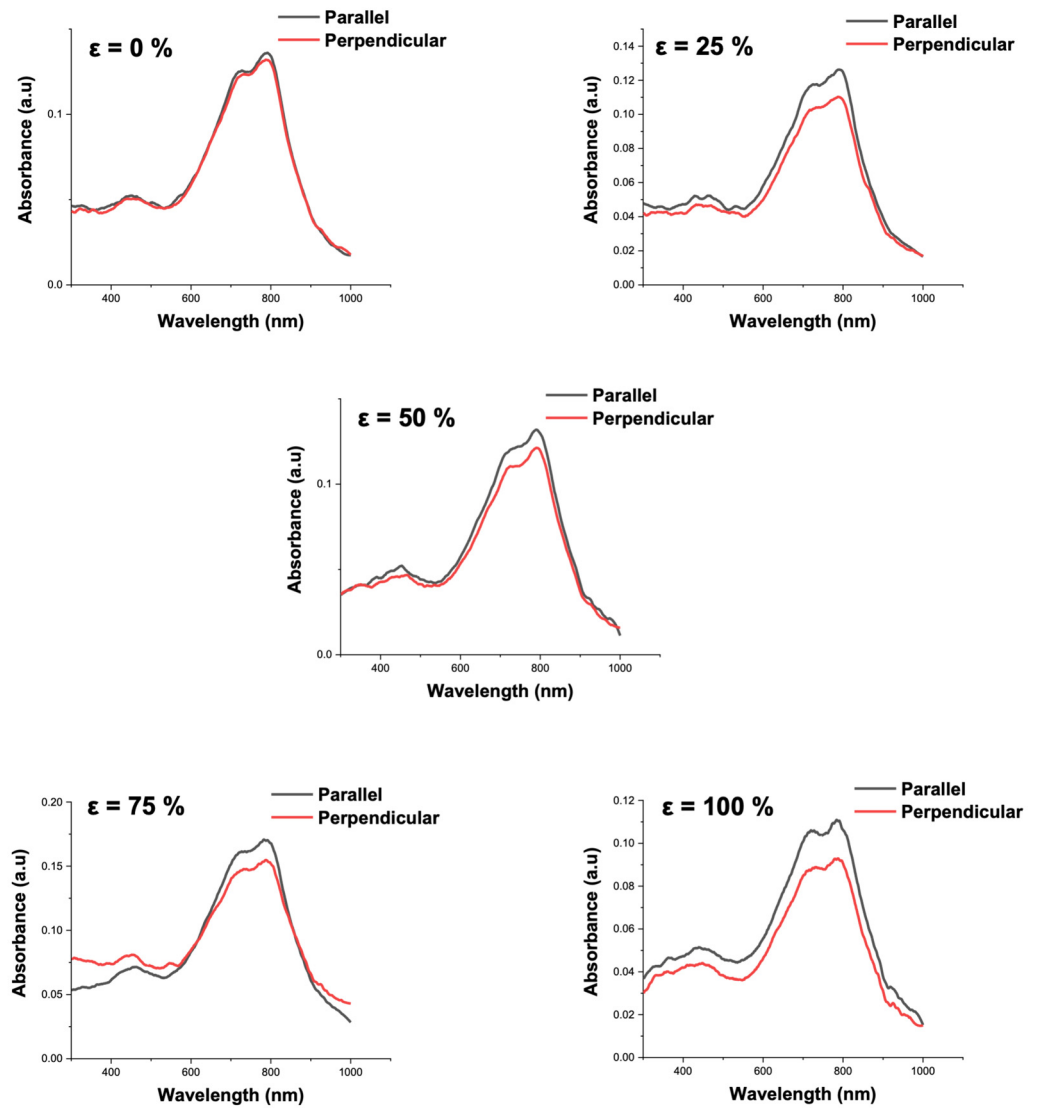


Figure S11. Polarized UV-vis spectra of LPE/P(DPPTVT):LPE blend films with 25 wt.% LPE stretched at different percent strains, with the polarization direction of light parallel (0° , black trace) and perpendicular (90° , red trace) to the stretching direction.

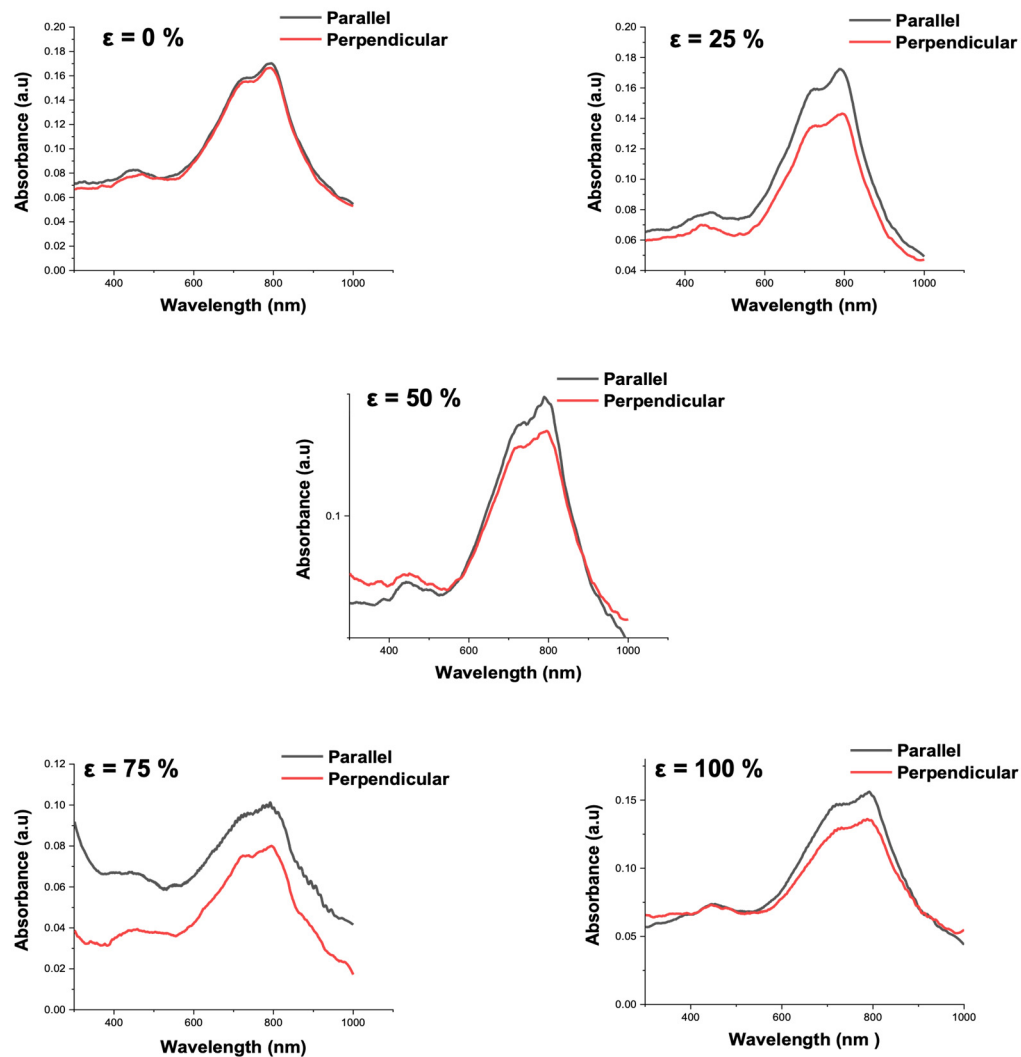


Figure S12. Polarized UV-vis spectra of P(DPPTVT):LPE blend films with 50 wt.% LPE stretched at different percent strains, with the polarization direction of light parallel (0° , black trace) and perpendicular (90° , red trace) to the stretching direction.

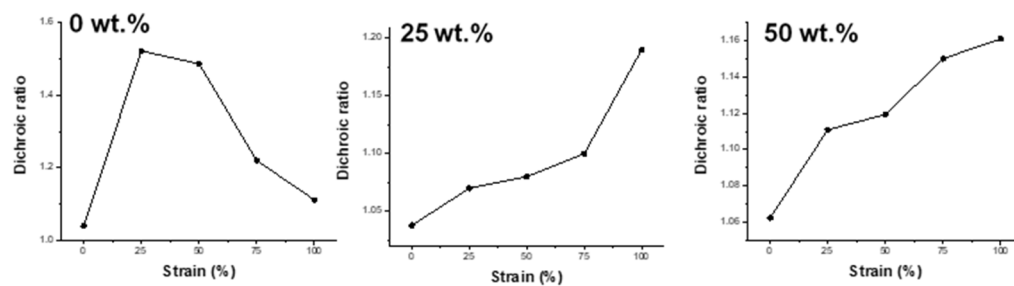


Figure S13. Dichroic ratios of the P(DPPTVT):LPE blend films as a function of strain applied determined by polarized UV-vis spectroscopy.

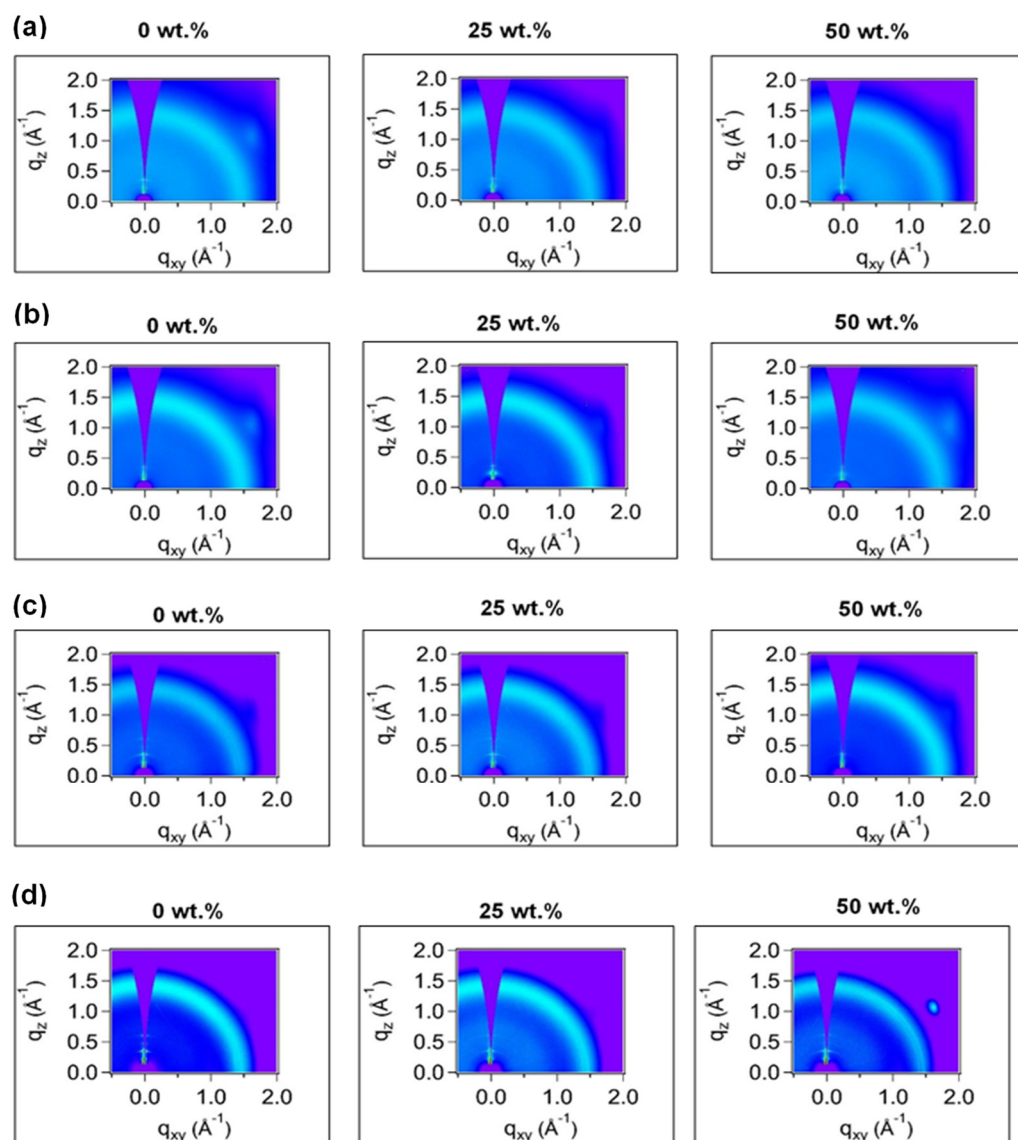


Figure S14. GIWAXS 2D patterns of P(DPPTVT):LPE blend films under: (a) 30% strain parallel, (b) 100% strain parallel, (c) 30% strain perpendicular, and (d) 100% strain perpendicular to the incident X-ray direction

Table S2. Average (μ_h^{avg}) and maximum hole mobilities (μ_h^{max}), threshold voltages (V_{th}), and I_{ON}/I_{OFF} ratios for OFETs fabricated using pre-stretched (0 and 25% strain) polymer blend films (0 to 50 wt.% LPE). The device performances were averaged from 5 devices and W/L represents channel width/length.

Sample	Direction	Strain %	W/L	μ_h^{avg}/μ_h^{max} ($\text{cm}^2 \text{V}^{-1} \text{s}^{-1}$)	I_{ON}/I_{OFF}^{avg}	V_{th}^{avg} (V)
0 wt. %	Parallel	0	10	$0.0089 \pm 0.003/0.0130$	10^6	-2.29 ± 0.85
		25	10	$8.147 \times 10^{-7} \pm 5.391 \times 10^{-6}$ $/1.601 \times 10^{-6}$	10^6	-14.90 ± 7.23
	Perpendicular	0	10	$0.0089 \pm 0.003/0.0130$	10^6	-2.29 ± 0.85
		25	10	$1.160 \times 10^{-6} \pm 8.241 \times 10^{-7}$ $/2.100 \times 10^{-6}$	10^6	-11.24 ± 1.22
25 wt. %	Parallel	0	10	$0.0085 \pm 0.0021/0.001$	10^6	-6.59 ± 0.86
		25	10	$3.240 \times 10^{-6} \pm 1.672 \times 10^{-6}$ $/5.655 \times 10^{-6}$	10^6	-13.20 ± 6.09
	Perpendicular	0	10	$0.0085 \pm 0.0021/0.001$	10^6	-6.59 ± 0.86
		25	10	$4.108 \times 10^{-6} \pm 3.757 \times 10^{-6}$ $/9.617 \times 10^{-6}$	10^6	-7.02 ± 4.70
50 wt. %	Parallel	0	10	$0.0129 \pm 0.0028/0.017$	10^6	-3.48 ± 5.12
		25	10	$0.0023 \pm 0.001/0.004$	10^6	-4.13 ± 4.68
	Perpendicular	0	10	$0.0129 \pm 0.0028/0.017$	10^6	-3.48 ± 5.12
		25	10	$0.0028 \pm 0.001/0.004$	10^6	-2.16 ± 0.50

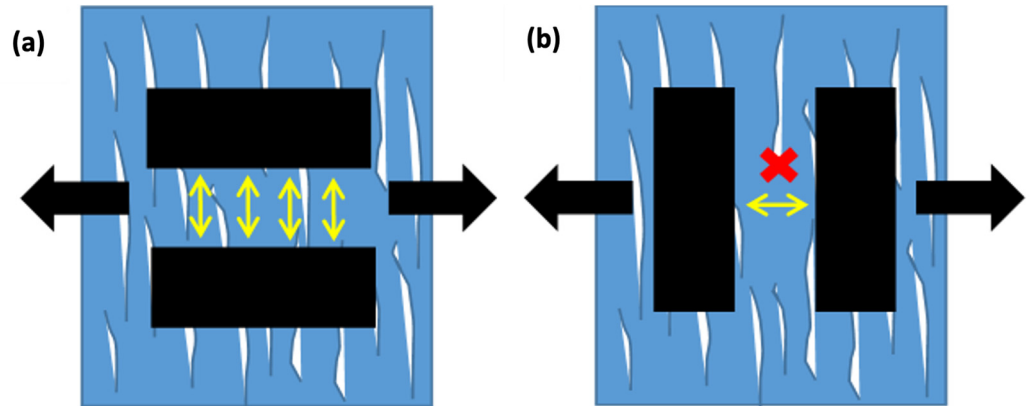


Figure S15. Schematic diagram illustrating the charge transport pathways (yellow arrows) between top electrodes when they are a: parallel or b: perpendicular to the stretching direction (black arrows).

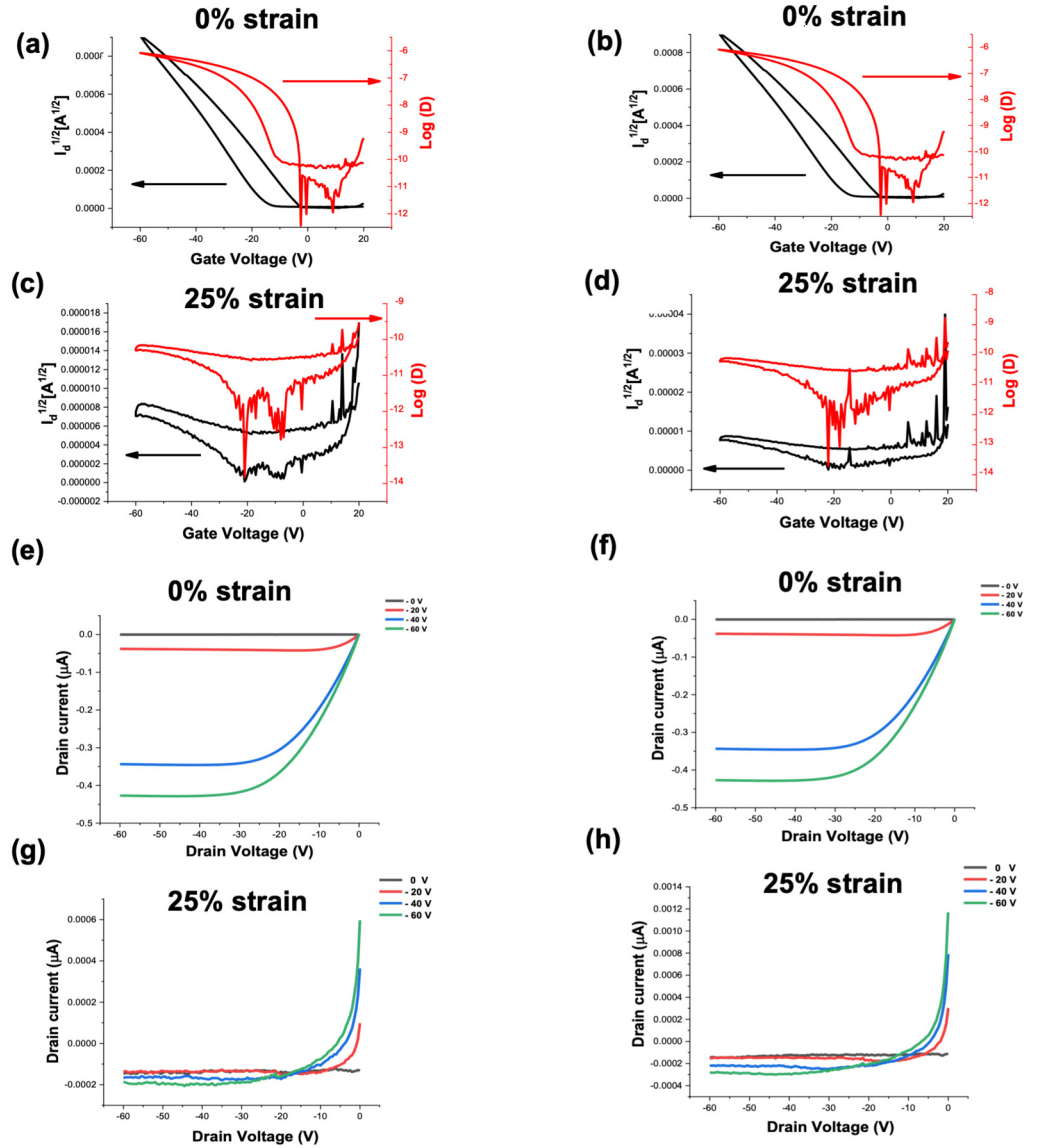


Figure S16. Transfer (a)–(d) and output (e)–(h) curves for OFET devices fabricated using transferred pre-stretched P(DPPTVT) films on SiO₂ at different applied strains: (a) and (e) 0% strain parallel to the charge transport, (b) and (f) 0% strain perpendicular to the charge transport, (c) and (g) 25% strain parallel to the charge transport, and (d) and (h) 25% strain perpendicular to the charge transport. No annealing treatment was performed for these measurements and $V_d = -60V$.

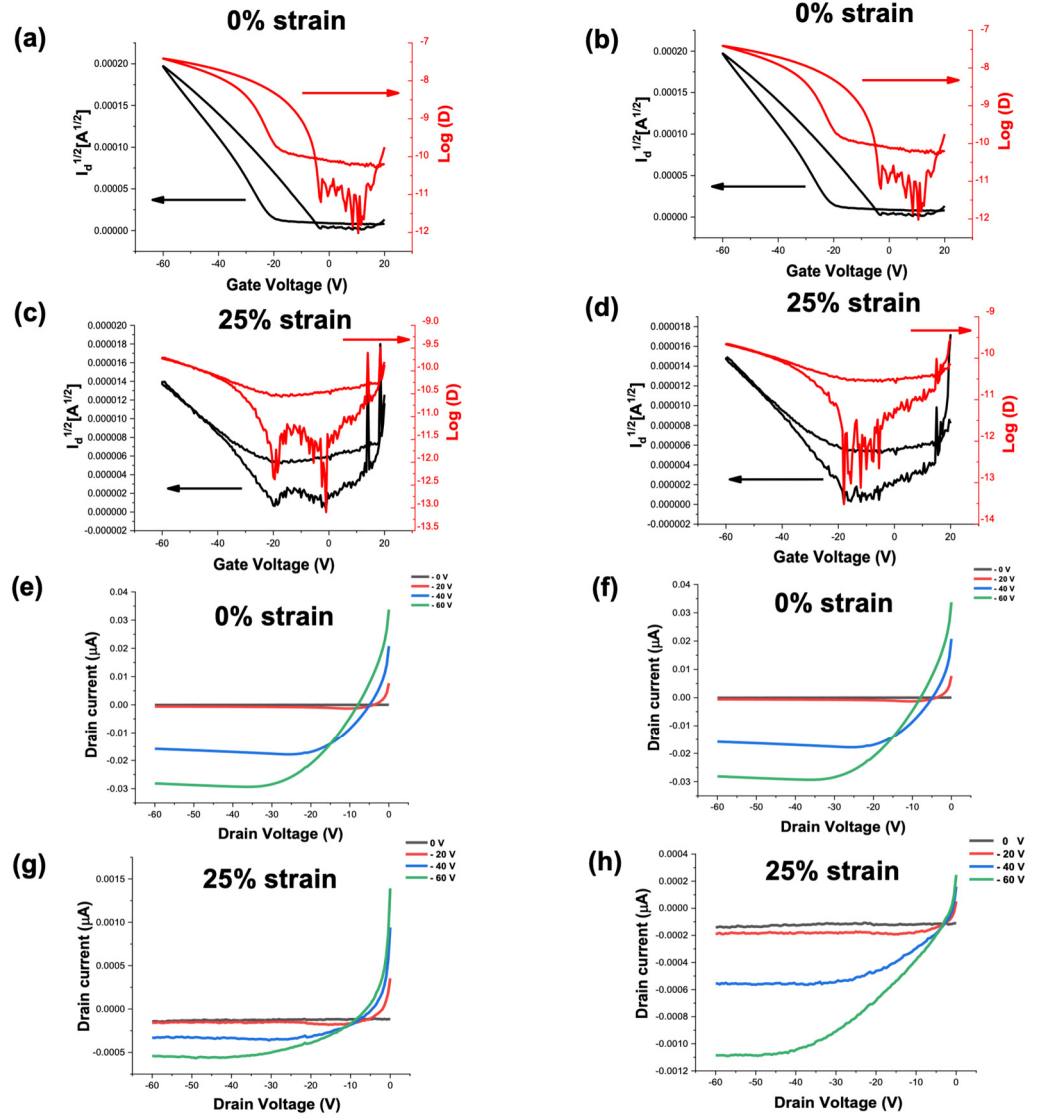


Figure S17. Transfer (a)–(d) and output (e)–(h) curves for OFET devices fabricated using transferred pre-stretched P(DPPTVT) films with 25 wt.% LPE on SiO₂ at different applied strains: (a) and (e) 0% strain parallel to the charge transport, (b) and (f) 0% strain perpendicular to the charge transport, (c) and (g) 25% strain parallel to the charge transport, and (d) and (h) 25% strain perpendicular to the charge transport. No annealing treatment was performed for these measurements and $V_d = -60V$.

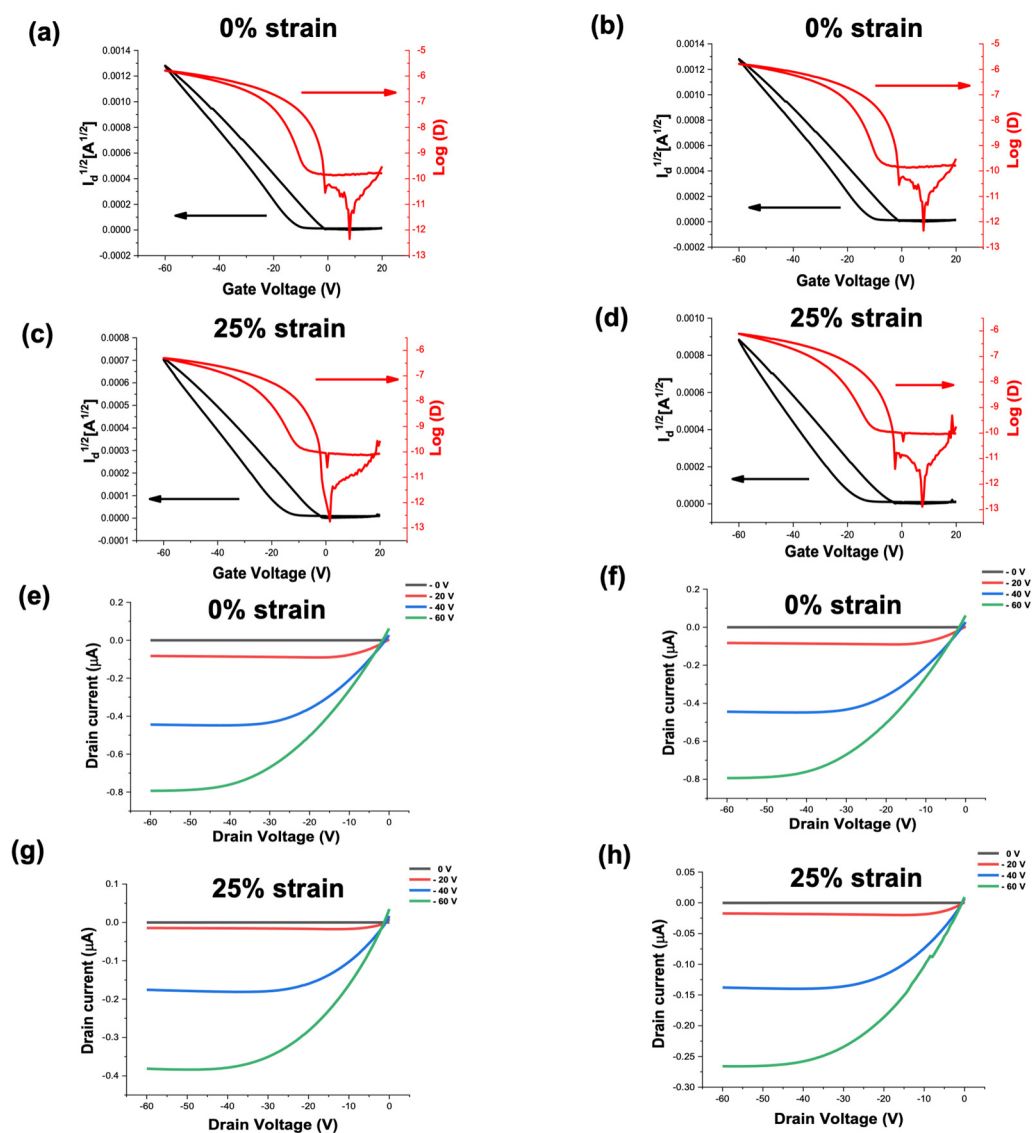


Figure S18. Transfer (a)–(d) and output (e)–(h) curves for OFET devices fabricated using transferred pre-stretched P(DPPTVT) films with 50 wt.% LPE on SiO₂ at different applied strains: (a) and (e) 0% strain parallel to the charge transport, (b) and (f) 0% strain perpendicular to the charge transport, (c) and (g) 25% strain parallel to the charge transport, and (d) and (h) 25% strain perpendicular to the charge transport. No annealing treatment was performed for these measurements and $V_d = -60$ V.

References

1. Zalesskiy, S. S.; Ananikov, V. P. Pd₂(dba)₃ as a Precursor of Soluble Metal Complexes and Nanoparticles: Determination of Palladium Active Species for Catalysis and Synthesis. *Organometallics* **2012**, 31 (6), 2302–2309.
2. Yu, H.; Park, K. H.; Song, I.; Kim, M.-J.; Kim, Y.-H.; Oh, J. H. Effect of the Alkyl Spacer Length on the Electrical Performance of Diketopyrrolopyrrole-Thiophene Vinylene Thiophene Polymer Semiconductors. *J. Mater. Chem. C* **2015**, 3 (44), 11697–11704.
3. Ito, Y.; Virkar, A. A.; Mannsfeld, S.; Oh, J. H.; Toney, M.; Locklin, J.; Bao, Z. Crystalline Ultrasoother Self-Assembled Monolayers of Alkylsilanes for Organic Field-Effect Transistors. *J. Am. Chem. Soc.* **2009**, 131 (26), 9396–9404.